Kashani, M. M., Alagheband, P., Khan, R., & Davis, S. A. (2015). Impact of corrosion on low-cycle fatigue degradation of reinforcing bars with the effect of inelastic buckling. International Journal of Fatigue, 77, 174–185. 10.1016/j.ijfatigue.2015.03.013

Impact of corrosion on low-cycle fatigue degradation of reinforcing bars with the effect of inelastic buckling

Mohammad M. Kashani, Peyman Alagheband, Rafid Khan, Sean Davis

PII: S0142-1123(15)00078-X
DOI: http://dx.doi.org/10.1016/j.ijfatigue.2015.03.013
Reference: JIJF 3548

To appear in: *International Journal of Fatigue*

Received Date: 17 January 2015
Revised Date: 11 March 2015
Accepted Date: 12 March 2015

Please cite this article as: Kashani, M.M., Alagheband, P., Khan, R., Davis, S., Impact of corrosion on low-cycle fatigue degradation of reinforcing bars with the effect of inelastic buckling, *International Journal of Fatigue* (2015), doi: http://dx.doi.org/10.1016/j.ijfatigue.2015.03.013

Impact of corrosion on low-cycle fatigue degradation of reinforcing bars with the effect of inelastic buckling

Mohammad M. Kashani[1], Peyman Alagheband[2], Rafid Khan[3], Sean Davis[4]

Abstract

The combined effect of inelastic buckling and chloride induced corrosion damage on low-cycle high amplitude fatigue life of embedded reinforcing bars in concrete is investigated experimentally. A total of forty eight low-cycle fatigue tests on corroded reinforcing bars varied in percentage mass loss, strain amplitudes and buckling lengths are conducted. The failure modes and crack propagation are investigated by fractography of fracture surfaces using scanning electron microscope. The results show that the inelastic buckling, percentage mass loss and nonuniform corrosion pattern are the main parameters affecting the low-cycle fatigue life of reinforcing bars. It was found that the fatigue life of corroded reinforcing bars combined with inelastic buckling has a significant path dependency. The results show that in some cases the number of cycles to failure of corroded bars under constant amplitude fatigue test is increased.

Keywords: Low-cycle fatigue, corrosion, buckling, cyclic behaviour, reinforcing steel, stress-strain relation

1. Introduction

Corrosion of reinforcing steel is the most significant structural deficiency in aging bridges located in chloride laden environment. Many of these bridges are also located in regions with high seismic activities. These structures experience dynamic/cyclic loading due to earthquake over their service life. Furthermore, the current design approach allows reinforced concrete

[1]Lecturer, University of Bristol, Dept. of Civil Engineering University of Bristol, Bristol, BS8 1TR, United Kingdom (corresponding author), E-mail: mehdi.kashani@bristol.ac.uk
[2]MSc Student, University of Surrey, Dept. of Civil Engineering, formerly BEng student, University of Bristol
[3]MEng student, University of Bristol, Dept. of Civil Engineering
[4]Senior Lecturer, University of Bristol, School of Chemistry

(RC) structures dissipate energy during large earthquake events by occurring plastic hinges in beams and columns. The inelastic cyclic deformation in plastic hinge regions during large earthquakes results in a significant tension and compression strain reversals. Among RC components, bridges piers are the most vulnerable components in earthquake due to the simple structural system of bridges. Moreover, there is a large number of existing bridges around the world that were designed prior to the modern seismic design codes and therefore they are not properly detailed for seismic loading. These aging structures are also suffering from long-term material deterioration.

One of the most common type of failure modes of RC bridge piers that has been observed in real earthquakes and experimental testing is the buckling of vertical reinforcement which is then followed by fracture of reinforcement in tension due to low-cycle high amplitude fatigue failure [1,2]. Meda et al., Ou et al. and Ma et al. [3-5] have investigated the effect of corrosion on the nonlinear response of RC beams and columns subject to cyclic loading experimentally. The results from these experimental studies show that non-uniform pitting corrosion affects the global response of corroded RC elements subject to cyclic loading. This is mainly due to the influence of corrosion on premature buckling and low-cycle fatigue life of corroded bars.

The low-cycle fatigue life of uncorroded reinforcing bars without the effect of buckling has been studied by other researchers [6-10]. Kashani et al. [11] studied the effect of inelastic buckling on low-cycle fatigue life of uncorroded reinforcing bars experimentally. [12] and [13] investigated the effect of corrosion on low-cycle fatigue life of reinforcing bars without the effect of buckling. More recently, Kashani et al. [14,15] investigated the impact of corrosion on inelastic buckling and nonlinear cyclic response of reinforcing bars experimentally. Kashani [16-18] studied the impact of corrosion pattern on inelastic buckling and cyclic response of reinforcing bars using a detailed nonlinear finite element analysis. The

results of previous research other researchers [15-20] show that the combined effect of corrosion and inelastic buckling has a significant impact on premature fracture of reinforcing bars under cyclic loading. However, there has not been any experimental testing to explore and quantify the combined effect of corrosion and inelastic buckling on low-cycle fatigue degradation of reinforcing bars.

This paper explores the combined effect of corrosion damage and inelastic buckling on low-cycle fatigue life of reinforcing bars experimentally. The effect of buckling and corrosion on the total hysteretic energy dissipation capacity and the number of cycles to failure are investigated. Using scanning electron microscope the fractography of fracture surfaces is studied. The experimental results show that the low-cycle fatigue life of corroded reinforcing bars with the effect of inelastic buckling is greatly influenced by loading history and therefore, has a significant path dependency. Finally, a comparison between the result of this experiment and the experimental results observed by other researchers where buckling was not included is made. The comparison of result shows that the path dependency is less significant in corroded bars where buckling is not an issue. The results of this experiment suggests that there is need for further experimental studies to investigate the impact of loading history on low-cycle fatigue life of corroded bars with the effect of inelastic buckling. However, given the significant paucity in the literature and the complexity of problem, the experimental results reported in this paper provide an insight into this important problem and creates an opportunity for other researchers to take this further in the future research.

2. Experimental programme

2.1. Specimen preparation and corrosion procedure

In order to realistically simulate the corrosion of steel reinforcement embedded in concrete a total of four reinforced concrete specimens were cast. Each specimen dimensioned

250×250×700mm incorporated 12 number 12mm diameter B500 British manufactured reinforcing bars [21] as shown in Fig. 1. The concrete mix was designed to have a mean compressive strength of 30MPa at 28 days with a maximum aggregate size of 12mm. The specimens were cast with a nominal cover of 25mm.

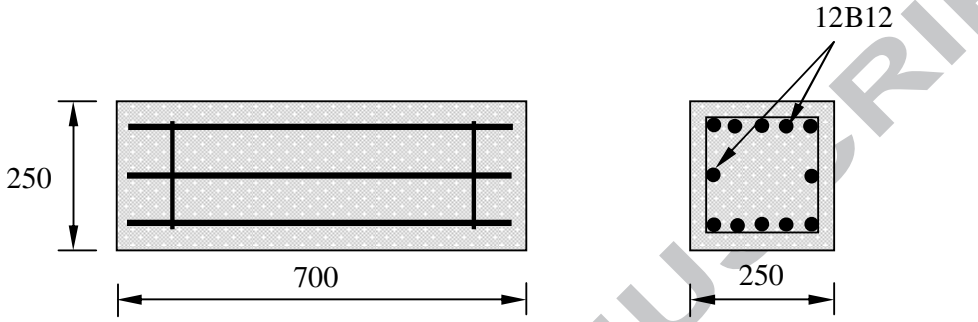

Fig. 1. RC specimens prepared for the accelerated corrosion of reinforcement bars

An accelerated corrosion procedure was used to simulate long term corrosion. The concept of using external currents is simple and consists of forming an electrochemical circuit using an external power supply. The reinforcing bars act as the anode in the cell and an external material acts as the cathode as shown in Fig. 2(a). An example of corroded specimen after accelerated corrosion procedure is shown in Fig. 2(b).

The time required to get the desired corrosion level was estimated using Faraday's 2nd Law of Electrolysis. After corrosion simulation, the concrete specimens (shown in Fig. 2) were broken open and the corroded bars were carefully removed from the concrete. To ensure that the concrete was completely removed from the corroded bars, a mechanical cleaning process using a bristle brush was used, in accordance with ASTM G1-03 [22]. The corroded bars were then washed with tap water and dried. The brushing and washing process was then repeated a second time. An example of corroded reinforcement after cleaning process is shown in Fig. 3. It should be noted that the same brushing process was applied to the

uncorroded control specimens and it was found that the effect of brushing on the mass loss of base material is negligible.

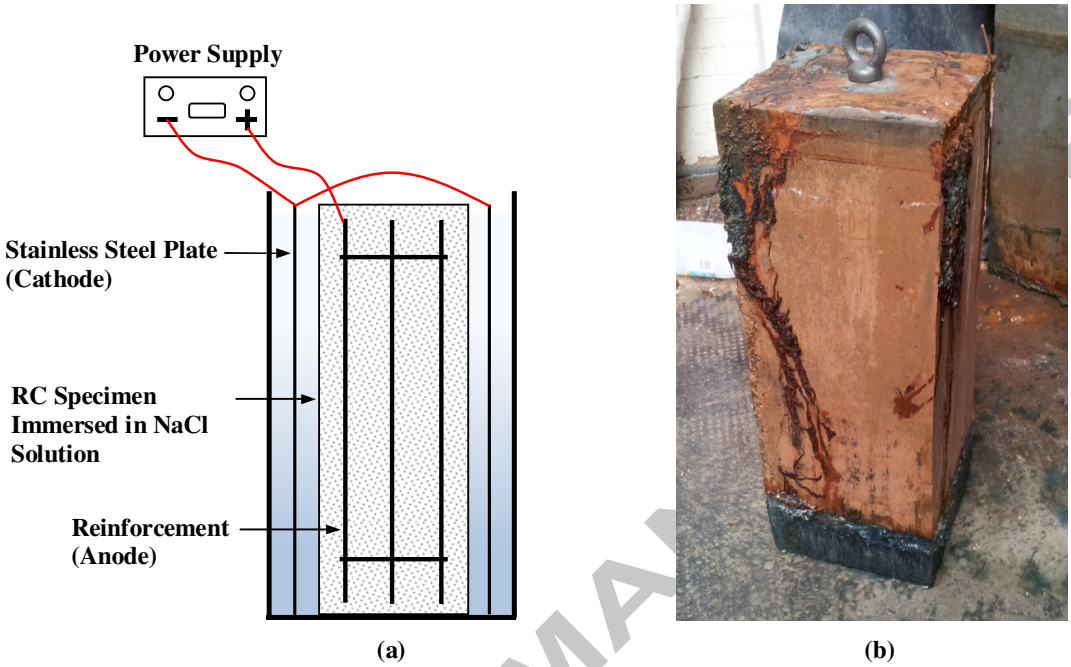

Fig. 2. Corrosion Procedure: (a) schematic illustration of accelerated corrosion procedure, and (b) corroded specimen after accelerated corrosion procedure

Fig. 3. Corroded reinforcement after cleaning process

Assuming a uniform mass loss, the mean reduced diameter of the reinforcement can be estimated using Eq. (1) which gives an average residual diameter of reinforcement relative to the mass loss:

$$D' = D_0\sqrt{1-\gamma} \tag{1}$$

where D_0 is the initial diameter of the uncorroded bar and γ is the mass loss ratio based on Eq. (2):

$$\gamma = \left(\frac{m_0 - m}{m_0}\right) \tag{2}$$

where m_0 is the mass per unit length of the original steel bar, m the final mass per unit length of the steel bar after removal of the corrosion products. A more detailed discussion of the accelerated corrosion procedure, mechanical properties of tested reinforcement and the influence of corrosion on mechanical properties of corroded bars can be found in Kashani *et al.* [14].

2.2. Low-cycle high amplitude fatigue test

A total of forty eight low-cycle fatigue tests are conducted on corroded reinforcing bars with different buckling lengths and strain amplitudes. It is well known that the buckling length of the vertical reinforcing bars inside RC columns is a function of the stiffness of horizontal tie reinforcement [16]. Therefore, slenderness ratios for the experiment are chosen based on the common observed buckling modes of vertical reinforcement in RC columns as report in [16]. The slenderness ratio is defined by the *L*/*D* ratio where *L* is the length and *D* is the bar diameter. The *L*/*D* ratios tested in this experiment are 5, 10 and 15.

A 250kN universal testing machine with hydraulic grips was used for the low-cycle fatigue testing of the reinforcing bars. The machine used an integral Linear Variable Displacement Transducer (LVDT) to measure the displacement of the grips. A displacement control loading protocol with zero mean strain using a sine wave loading pattern with constant amplitude is used in the low-cycle fatigue tests. The strain rate is set to 0.005strain/sec throughout the experiment. The total strain amplitudes used in the low-cycle fatigue tests are 1%, 2%, 3%,

4% and 5%. A picture of a test specimen placed in the universal testing machine is shown in Fig. 4. It should be noted that the failure of the specimen is taken to be the point at which the bar is completely fractured.

Fig. 4. Low-cycle fatigue test setup of a corroded bar with *L*/*D* = 5

3. Experimental results and discussion

3.1 Impact of corrosion on cyclic stress-strain response

Fig. 5 shows hysteretic loops of corroded bars with different *L*/*D* ratios and percentage mass losses under 4% strain amplitude fatigue test. It should be noted that in this paper the stress of corroded bars is calculated assuming a uniform volumetric mass loss using Eq. (1) (mean stress) and the strain is the average strain over the length (*L*) of bars (mean strain). Comparing Fig 5(a) (*L*/ *D* = 5) with (b) and (c) (*L*/ *D* = 10 and 15) shows that inelastic buckling has a significant impact on cyclic stress-strain response of reinforcing bars. It is also evident that the cyclic degradation is much quicker in bars with bigger *L*/*D* ratios. This is due to the impact of geometrical nonlinearity on the stress-strain response of reinforcing bars. As it is shown in Fig. 5(a) the stress-strain response of uncorroded bars with *L*/*D* = 5 is symmetrical in tension and compression. This is because the inelastic buckling is not an issue

in these bars. Previous research has confirmed that buckling is not an issue in reinforcing bars with $L/D < 6$ [14,15]. However, once reinforcing bars start corroding the nonuniform corrosion over the length of corroded bars changes the effective slenderness ratio (L/D) of these bars. Therefore, inelastic buckling affects the stress-strain response of these bars as shown in Fig. 5(a).

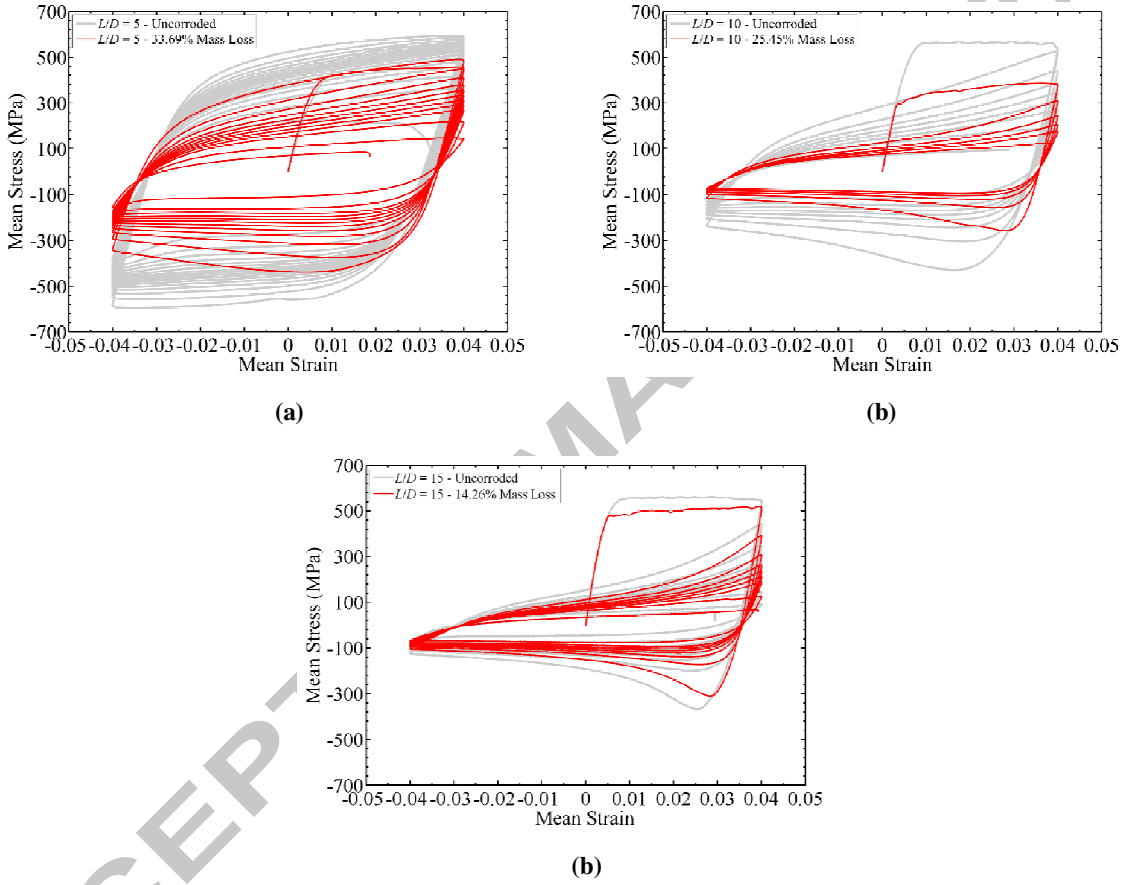

Fig. 5. Impact of corrosion on cyclic stress-strain response of reinforcing bars: (a) L/D = 5 (b) L/D = 10 (c) L/D = 15

The strain amplitude is the most important parameter affecting the low-cycle fatigue of materials. The experimental results show that the influence of strain amplitude increases by increasing the L/D ratios of bars. Fig. 6 shows the uncorroded control test specimens with L/D = 10 after low-cycle fatigue tests at different strain amplitudes. Comparison of the bars tested at 1% and 4% strain amplitude shows that fracture mechanism of these bars are

different due to the second order effect after buckling. This is because the strain amplitude across the critical cross section of bars subject to 1% strain amplitude fatigue test is almost uniform. However, in 4% strain amplitude fatigue tests the strain amplitude at the inner face of buckled bars is greater than the outer face. This is due to the second order effect (axial plus bending strain) which is very sensitive to the lateral deformation in post-buckling region. Therefore, the low-cycle fatigue degradation of reinforcing bars is significantly affected by inelastic buckling.

Fig. 6. Control bars with *L/D* = 10 after low-cycle fatigue tests at different strain amplitude

3.2 Impact of corrosion on hysteretic energy dissipation

The total dissipated energy to failure is one of the important low-cycle fatigue parameter that needs to be evaluated. This is a good representation of the energy storage capacity of the material during seismic event. The total hysteretic energy loss of the test specimens (E'_t) is calculated as sum of the area confined within the hysteretic loops using Green's theorem. The calculated dissipated energy of each corroded test specimen is normalised to its

corresponding uncorroded test specimen (E_t). Fig. 7 shows the impact of corrosion on normalised dissipated energy of corroded test specimens.

Earlier research by Kashani et al. [11] showed that inelastic buckling has a significant impact of hysteretic energy dissipation of the reinforcing bars in incrementally increasing strain amplitude. However, Fig. 7 shows that corrosion has a more significant impact on energy dissipation capacity of bars with $L/D = 5$. Fig. 7 suggests that increasing the L/D ratio of test specimens reduces the impact of corrosion on energy dissipation capacity of corroded bars under constant amplitude fatigue test.

Fig. 7 also shows a big scatter in the experimental data. This is due to highly complex random nature of corrosion phenomenon. Previous research [14,15,18] showed that the distribution of nonuniform pitting corrosion along the length of bars is the most important parameter affecting the nonlinear cyclic response of these bars. The distribution of pits also affects the buckling mechanism of corroded bars. Therefore, the energy dissipation capacity of corroded bars with highly localised pitting corrosion is significantly less than a corroded bar with the uniform corrosion. It should be noted that the cyclic loading protocol used in [15] was a two cycle reversed symmetrical incrementally increasing strain amplitude history. This suggests that there is a path dependency in the cyclic/fatigue behaviour of corroded bars with the effect of buckling. This path dependency also affects the number of cycles to failure in corroded bars with the effect of buckling which is discussed in sections 3.3 of this paper.

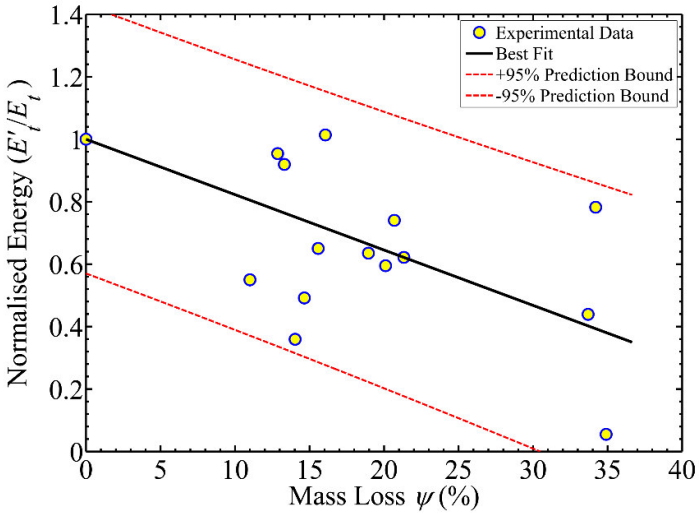

(a)

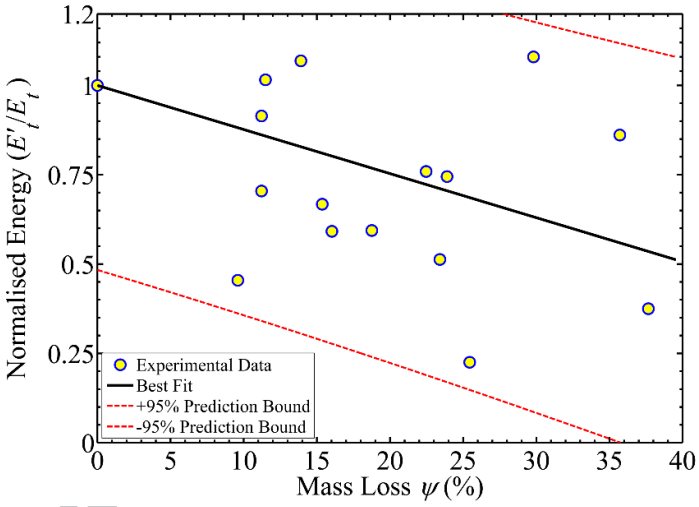

(b)

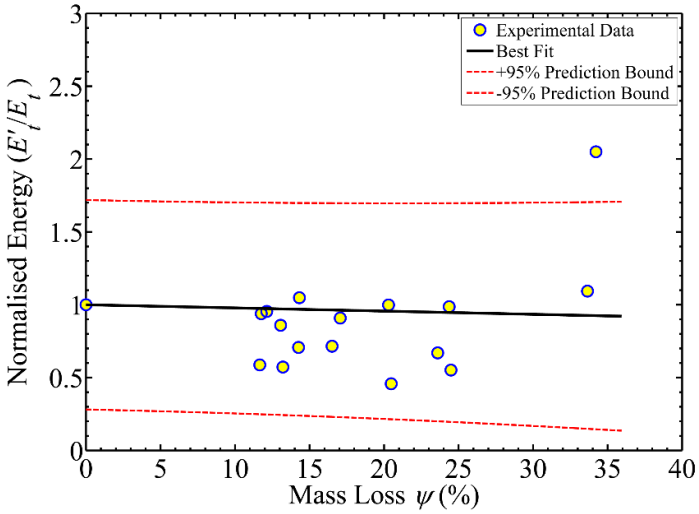

(c)

Fig. 7. Impact of corrosion on total hysteretic energy dissipation of reinforcing bars: (a) *L/D* = 5, (b) *L/D* = 10 and (c) *L/D* = 15

3.3 Impact of corrosion on the number of cycles to failure (low-cycle fatigue life)

The low-cycle fatigue life of reinforcing bars without the effect of buckling has been studied by several researchers [6-10]. The Coffin-Manson [23] model is one of the most popular methods among researchers as they are easy to be used implemented in nonlinear material models [24] of finite element packages for seismic analysis of civil engineering structures such as OpenSees [25].

The Coffin-Manson equation uses the strain life approach to model the low-cycle fatigue life of engineering materials. The plastic strain amplitude is the most important parameter affecting the low-cycle fatigue life of material. Therefore, Coffin-Manson model, as described in Eq. (1), relates the plastic strain amplitude (ε_p) to the fatigue life.

$$\varepsilon_p = \varepsilon'_f \left(2N_f\right)^c \tag{3}$$

where, ε'_f is the ductility coefficient i.e. the plastic fracture strain for a single load reversal, c is the ductility exponent and $2N_f$ is the number of half-cycles (load reversals) to failure. This section investigates the influence of corrosion on the number of half-cycles to failure ($2N_f$).

As expected, the degree of corrosion damage has a significant impact on the number of half-cycles to failure. The number of half-cycles to failure for each corroded specimen ($2N'_f$) is normalised to their corresponding uncorroded specimen ($2N_f$) and plotted versus percentage mass loss in Fig. 8. The detailed results are also tabulated in Appendix A of this paper. It should be noted that the results plotted in Fig. 8 are for all range of strain amplitudes.

The best linear fit to the experimental data in Fig. 8 shows that corrosion significantly reduces the number of half-cycles to failure for specimens with *L/D* = 5. However, it shows

that corrosion increases the number of half-cycles to failure for specimens with L/D = 10 and 15. For example comparing Fig 8(b) with Fig 7(b) shows that the total dissipated energy in specimens with L/D = 10 is significantly reduced by corrosion but the number of half-cycles to failure is increased. This is because corrosion reduced the diameter of reinforcing bars and therefore it affects the force displacement response. However, this indicates that the number of cycles to failure is significantly affected by the second order effect due to buckling (total strain = axial strain + bending strain). Furthermore, the 95% prediction bounds of the best linear fit shows that there is a big variation in the data which is due to the distribution of pitting corrosion along the length of corroded bars.

Earlier research by Kashani et al. [11] showed that the bar diameter and surface condition (ribbed or smooth) has a significant influence on the number of half-cycles to failure. They observed that as the bar diameter increases the number of half-cycles to failure decreases. Moreover, in ribbed bars the fatigue crack initiation starts at the root of the ribs due to stress concentration. As a result, the smooth bars experienced higher number of half-cycles to failure compare to ribbed bars. Therefore, if the corrosion is uniform along the length of corroded bars it is reducing the diameter and smoothing the surface of bars by removing the ribs. Further investigation and discussion about this phenomenon are available in sections 3.4 and 4 of this paper.

Other researchers [12,13] who conducted low-cycle fatigue tests on corroded bars found that the corrosion has more significant effect on the reduction of number of half-cycles to failure at low strain amplitude. In this experiment, similar results observed for the group of bars with L/D = 5 (Fig. 9(a)). However, it was found that in the group of bars with L/D = 10 and 15 the number of half-cycles to failure is generally increased by increasing the percentage mass loss and strain amplitudes (Fig. 9(b) and (c)). The detailed discussion and comparison of the results of this study with [12] and [13] are available in section 5 of this paper.

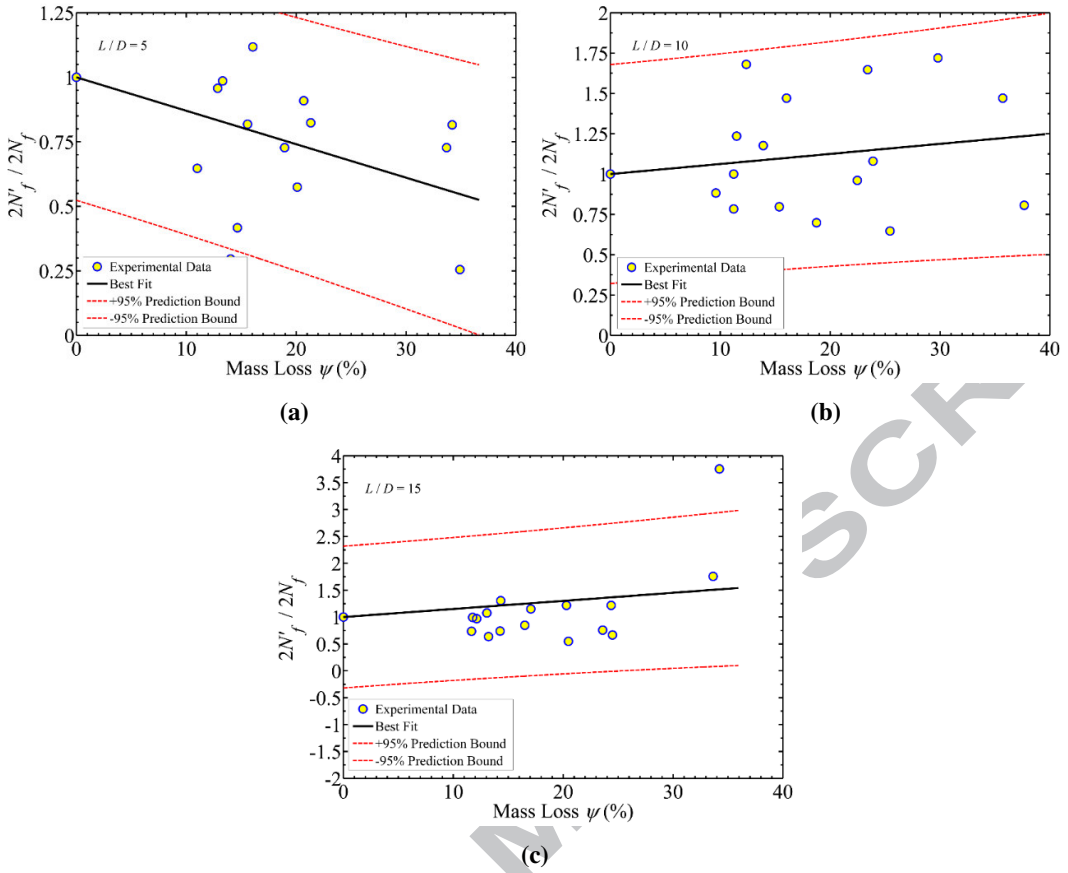

Fig. 8. Impact of corrosion on number of half-cycles to failure: (a) *L/D* = 5, (b) *L/D* = 10 and (c) *L/D* = 15

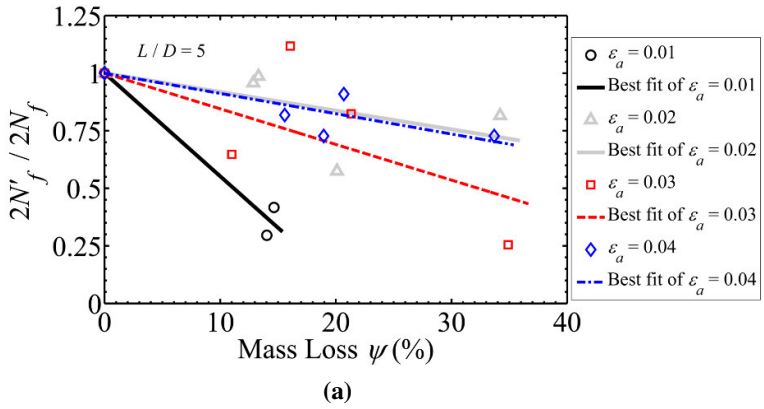

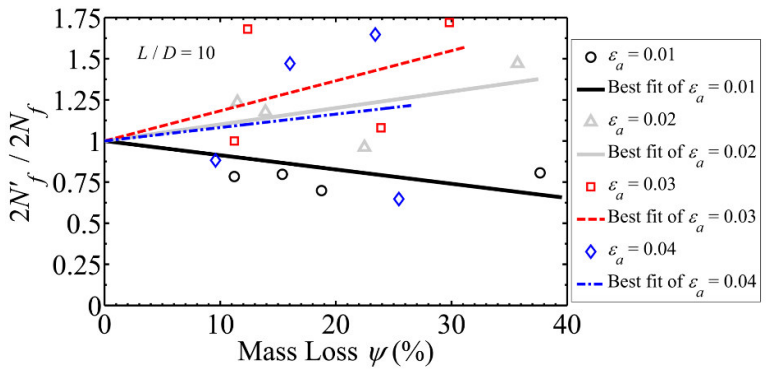

(b)

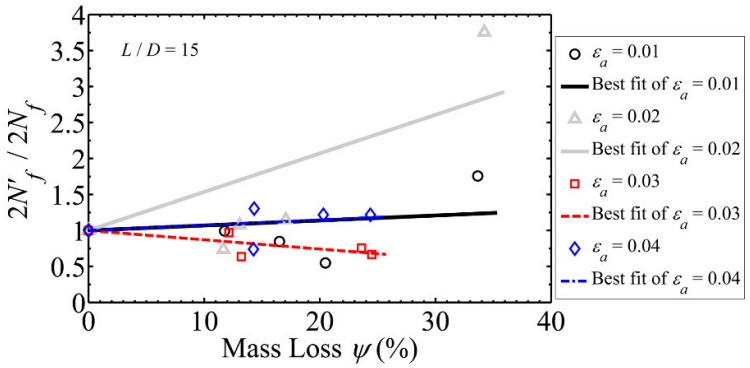

(c)

Fig. 9. Influence of strain amplitude on number of half-cycles to failure: (a) *L/D* = 5, (b) *L/D* = 10 and (c) *L/D* = 15

3.4 Impact of corrosion on cyclic stress loss

Fig. 10 shows the impact of corrosion on cyclic stress loss of reinforcing bars. It should be noted that the calculated stress in Fig. 10 is based on the average reduced area of corroded bars and is normalised to the yield stress of uncorroded specimen. Fig. 10(a) shows that as the corrosion damage increases in group of bars with *L/D* = 5, the number of cycles to failure decreases and cyclic stress degradation increases. However, Fig. 10(b) shows that a corroded bar with *L/D* = 15 and 14.26% mass loss can sustain a smaller number of cycles to failure than a corroded bar with the same slenderness ratio and 24.37% mass loss. Comparing Fig. 10(a) and (b) shows that (as expected) as the corrosion damage increases the normalised stress decreases which suggests that the corroded bars in Fig. 10(a) have irregular distribution of corrosion along the length of the bars. However, it is clear that the stress loss graphs of

both corroded bars in Fig. 10(b) are coinciding. This suggests that the distribution of corrosion pits along the length of the corroded bar with 24.37% mass loss is more uniform than the corroded bar with 14.26% mass loss. The Fig. 10(b) is one example of several cases where increasing percentage mass losses resulted in increasing the number of cycles to failure. Therefore, for better understanding the influence of corrosion on failure mechanisms of corroded bars a fractography of the fracture surfaces bars is conducted which is discussed in the section 4 of this paper.

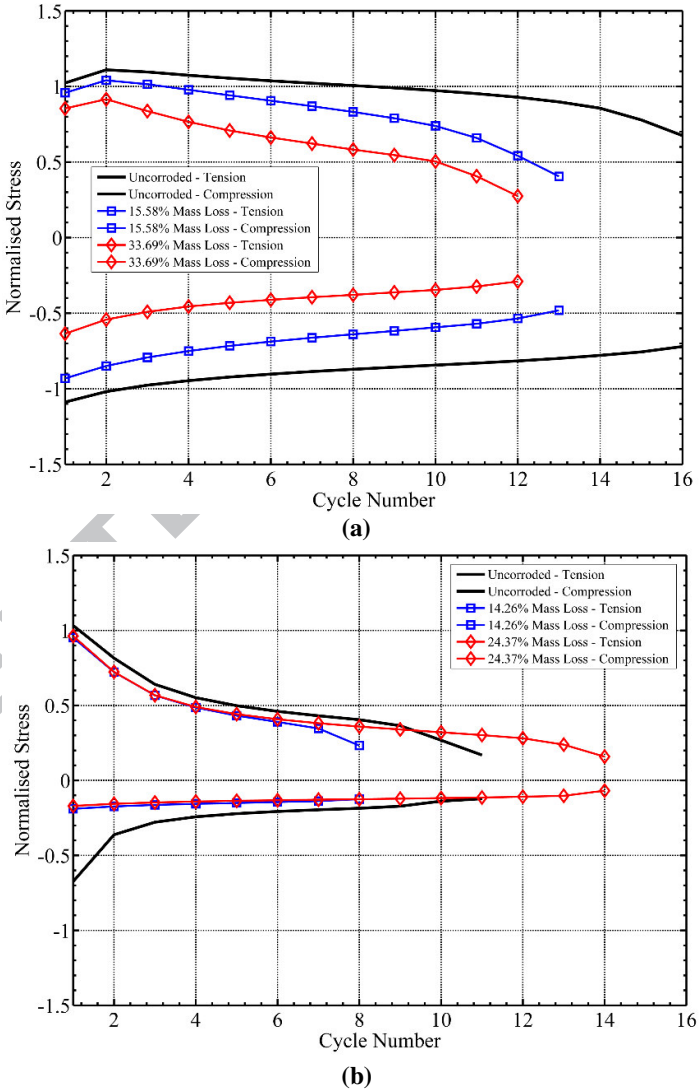

Fig. 10. Impact of corrosion on cyclic stress loss of reinforcing bars at 4% strain amplitude: (a) *L/D* = 5, (b) *L/D* = 15

4. Failure analysis and fractography of fracture surfaces using Scanning Electron Microscope (SEM)

Fig. 11 shows the pictures of three corroded bars after low-cycle fatigue test with 2% strain amplitude. Fig. 11(a) and (d) shows a corroded specimen with L/D = 5 and 34.20% mass loss. The number of half-cycles to failure in this specimen is reduced by about 20% compare to its corresponding uncorroded specimen. As it is clear in the picture the corrosion has a fairly irregular pattern along this bar. Fig. 11(b), (c), (e) and (f) shows two corroded specimens with L/D = 15. The corroded bar shown in Fig. 11(b) and (e) has 11.66% mass loss which failed much quicker than the corroded bar shown in Fig. 11(c) and (f) with 34.22% mass loss. In fact the low-cycle fatigue life of the corroded bar in Fig. 11(c) and (f) is about three times higher than its corresponding uncorroded specimen. In the group of bars with L/D = 10 and 15, several cases are observed that corrosion has increased the number of cycles to failure compare to the uncorroded specimens. The detailed results can be found in the Appendix A.

(a)

(b)

(c)

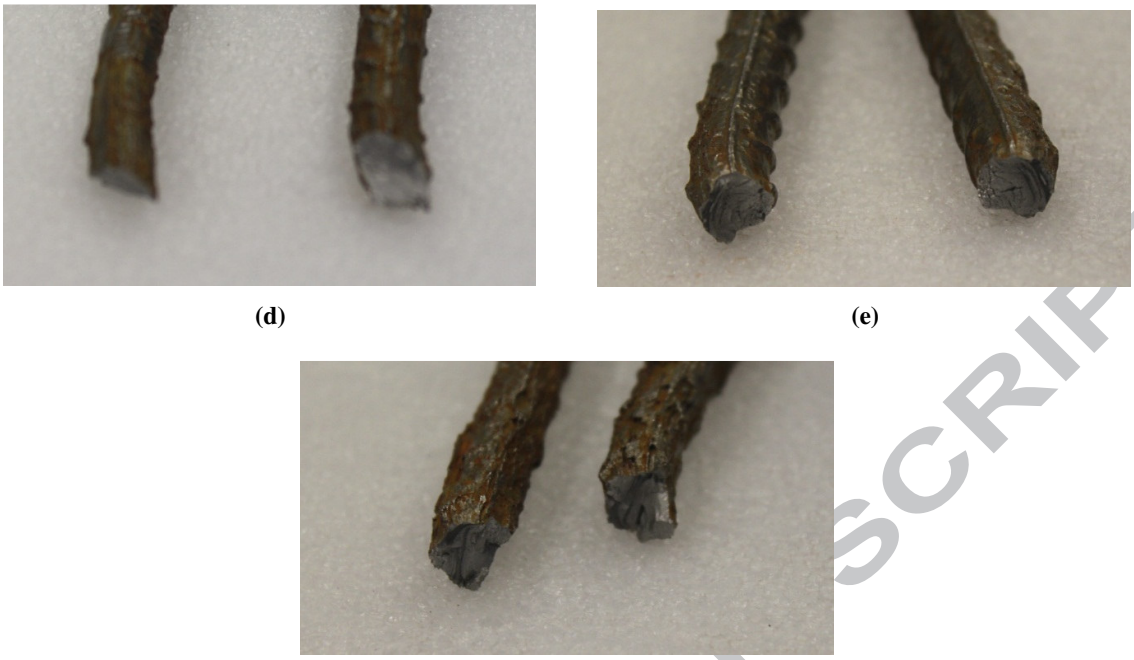

(d) **(e)**

(f)

Fig. 11. Photos of corroded bars after fracture under 2% strain amplitude: (a) and (d) *L*/*D* = 5 with 34.20% mas loss ($2N'_f$ / $2N_f$ = 0.82), (b) and (e) *L*/*D* = 15 with 11.76% mass loss ($2N'_f$ / $2N_f$ = 0.73) and (c) and (f) *L*/*D* = 15 with 34.22% mass loss ($2N'_f$ / $2N_f$ = 3.25)

Further investigation is conducted by fractography of the fractured surfaces. Fractographic analysis is done using a scanning electron microscope (SEM) in order to find the fatigue crack initiation sites and distinguish the propagation modes between the corroded bars. In general fatigue cracks normally initiated at the root of the ribs surface and propagated into the body of the bar normal to the bar axis in uncorroded specimens. This suggests that the maximum stresses lie in the longitudinal direction. Otherwise, the cracks would have grown along the root where the levels of stress concentrations are much higher than everywhere else. However, in corroded bars the location of crack initiation is significantly affected by the distribution of corrosion pits along the length of the bars.

Fig. 12 shows the fractographs of corroded bars previously shown in Fig. 11. Comparing Fig. 12(a) and (b) with Fig. 12(c) and (d) shows that the rough and light areas are associated with brittle and sudden fracture in this corroded bar with *L*/*D* = 5. It also shows that corrosion

resulted in some porosity around the surface of corroded bar which has a significant impact on crack initiation and the number of cycles to failure. Fig. 12(c-f) shows dark areas of striation that are associated with slower crack propagation and more ductile failure. However, comparing Fig. 12(c) and (d) with Fig. 12(e) and (f) shows that the corroded bar with lower mass loss ratio has experienced a more brittle failure mode. As discussed previously, this is due to the nonuniform corrosion pattern and buckling behaviour. It is also evident that corrosion induced porosity around the surface of corroded bars has a significant impact on the number of cycles to failure. Fig. 12(c) and (d) shows that the corroded bar with L/D = 15 and 11.76% mas loss had more significant porosity compare to Fig. 12(c) and (d) for a corroded bar with L/D = 15 and 34.22% mas loss. As a result the fatigue life of the corroded bar in Fig. 12(c) and (d) is much lower. This is a very important finding and requires further research to find the influence of mass loss ratio and accelerated corrosion technique on corrosion induced porosity around the surface of corroded bars.

Comparing the failure mode of corroded bars with L/D = 5 and 15 in Fig. 12(a-f) indicates that after crack initiation the whole of critical section in bars with L/D = 5 is in constant strain reversal (pure axial strain). However, in the group of bars with L/D = 15 the crack initiation is at the inner face of the buckled bar. If the bar is uncorroded this is in the middle (the location of plastic hinge) but in corroded bars this location varies depends on the distribution of pitting corrosion along the length of the bars. Therefore, the inner face of the buckled bar has much bigger strain amplitude than the outer face due to the combined axial plus bending strain. However, given the fatigue test is constant amplitude the outer face of the buckled bar experiences a residual plastic deformation after buckling. This is because when the bar is unload from compression and reload to tension to the same strain amplitude as the previous cycle the buckled bar doesn't completely straighten (Fig. 11(b) and (c)). In other words the change in the range of strain amplitude in the outer face of the buckled bar is significantly

less than the inner face. In this situation if the corroded bar has a localised pitting corrosion at this location, it fractures quickly after crack propagation from inner to outer face. However, if the corroded bar has a uniform corrosion, the fracture is similar to a bar with smaller diameter and smooth surface (without ribs) which is more ductile than the ribbed bars. This can be seen in Fig 12(e) and (f). Fig. 12(e) shows that after crack propagation there is a very dark area of striation towards the outer face of buckled bars. Comparing the failure modes of this experiment with earlier research by Kashani et al. [15] suggests that the failure mode of the corroded bars with effect of inelastic buckling under cyclic loading has a significant path dependency. This is an important finding which is out of the scope of this paper and is an area for future research.

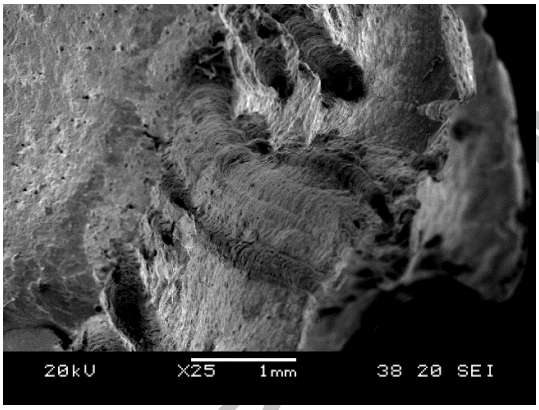

(a)

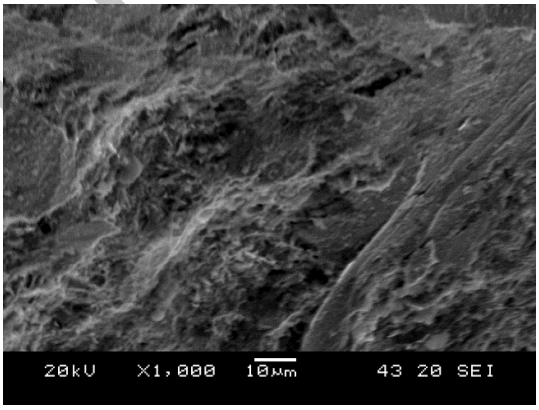

(b)

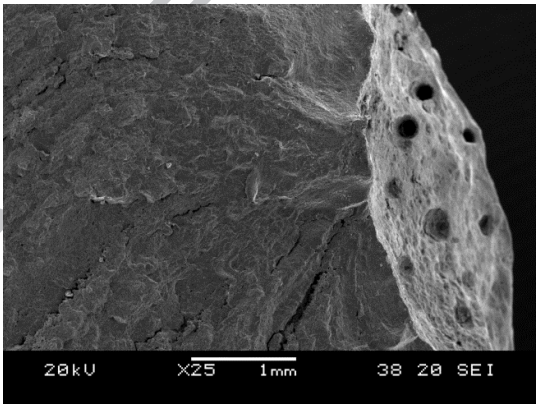

(c)

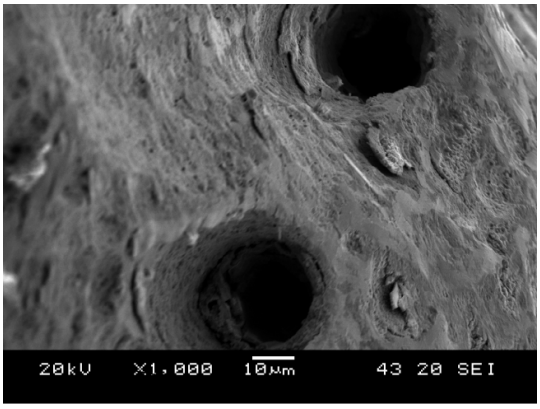

(d)

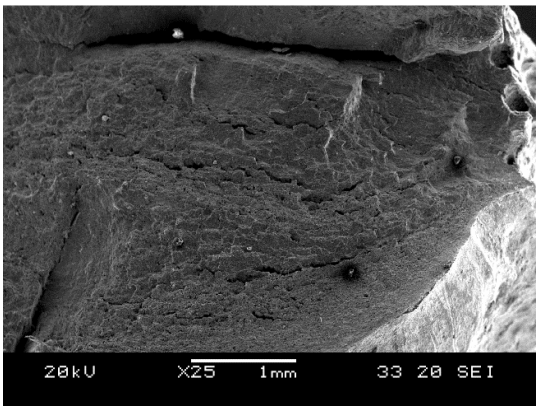

(e)

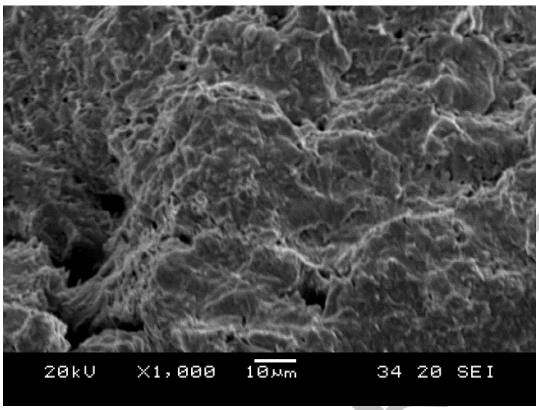

(f)

Fig. 12. SEM photos of fractured surface of corroded bars in Fig. 11: (a) and (b) *L/D* = 5 with 34.20% mas loss, (c) and (d) *L/D* = 15 with 11.76% mass loss and (e) and (f) *L/D* = 15 with 34.22% mass loss

5. Critical review and comparison of the observed results with previous experimental studies

Apostolopoulos [12] conducted low-cycle fatigue experiment on corroded reinforcing bars at 1%, 2.5% and 4% strain amplitudes. The test specimens had *L/D* = 6 and percentage mass losses ranged from 1% to 10%. The salt spray method was employed to accelerate the corrosion in the laboratory. Hawileh et al. [13] conducted low-cycle fatigue test on corroded reinforcing bars at 4%, 5%, and 6% strain amplitudes. In this experiment the specimens had *L/D* = 2 and percentage mass losses from 9% to 20%. The corrosion procedure was accelerated using 10% strong solution of sulfuric and nitric acids.

The test specimens in both of these experiments [12,13] were not corroded inside concrete. Therefore, the comparison of results shows that the scatter in the observed data in both of these experiments is less than the results observed in this paper. Comparing the results of [12] and [13] shows that there is a slight scatter in the data reported in [13] which specimens had higher percentage mass losses and fatigue test had bigger strain amplitudes. Fig. 13(a) and (b) shows the comparison of the best fit of all three experiments individually. It should be noted that only the results of the group of bars with *L/D* = 5 of this paper that didn't experience any

significant buckling are compared with [12] and [13]. The best fit of three experiments are shown in Fig. 13 individually. The parameters that are compared are normalised total dissipated energy and the normalised number of half-cycles to failure. Fig 13(a) and (b) shows that the corrosion has more significant impact at lower mass loss ratios. Fig. 13(c) and (d) shows the best of the combined observed data of all three experiment together. This suggests that as the percentage mass loss increases the scatter of data also increases. Therefore, as expected, the method of accelerated corrosion procedure and percentage mass loss have significant influence on the results. This finding is in a good agreement with the results obtained by [26]. Therefore, there is a need for further experimental studies to investigate the various parameters affecting the low-cycle fatigue life of corroded bars.

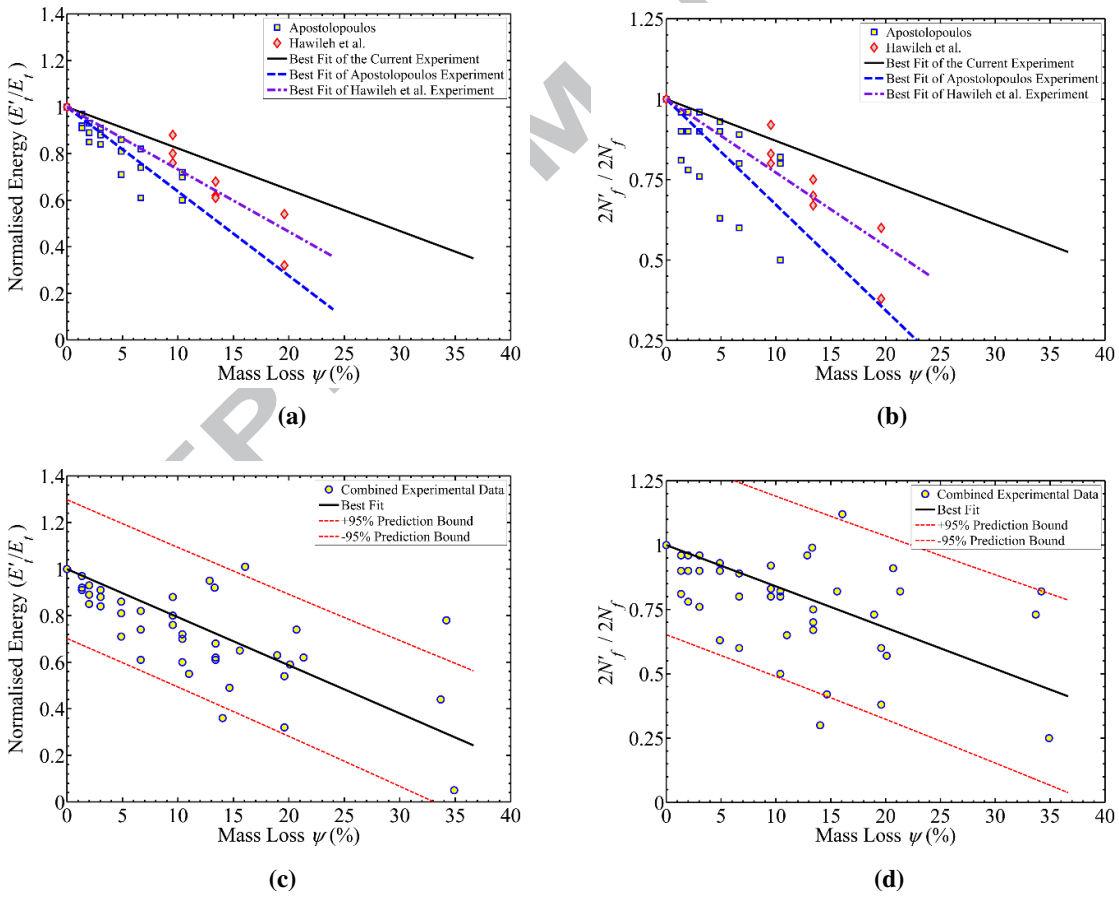

Fig. 13. Comparison of the results of this study for group of bars with *L*/*D* = 5 with other researchers: (a) comparison of the total hysteretic energy dissipation, (b) comparison of the number of half-cycles to

failure, (c) Impact of corrosion on total hysteretic energy dissipation for combined experimental data (current and other researchers) and (d) Impact of corrosion on the number of half-cycles to failure for combined experimental data

6. Conclusion

A total of forty eight constant amplitude low-cycle fatigue tests on corroded reinforcing bars with the effect of inelastic buckling are conducted. The test specimens were varied in lengths, percentage mass loss and strain amplitudes. Using SEM the fractography of fracture surfaces and failure mechanisms of test specimens are studied. The main outcomes of this study can be summarised as follows:

1) Corrosion has a significant impact on the cyclic stress-strain response of reinforcing bars. The uncorroded bars with L/D = 5 had a symmetrical stress-stress response in tension and compression. However, corrosion changes the effective slenderness ratio of these bars. Therefore, the cyclic response of these bars is affected due to the inelastic buckling.

2) The experimental results show that corrosion has a more significant impact on loss of energy dissipation capacity in the group of bars with L/D = 5 compare to the group of bars with L/D = 10 and 15.

3) It is observed that corrosion generally reduces the number of half-cycles to failure in the group of bars with L/D = 5. However, in several cases corrosion results in an increase in number of half-cycles to failure in the group of bars with L/D = 10 and 15.

4) The SEM results reveal that corrosion results in creation of a layer around the corded bars with significant porosity. These is need for further research to explore the influence of mass loss ratio and the accelerated corrosion technique on this porosity.

5) In several cases corrosion resulted in an increase in the number of half-cycles to failure. However, the same test specimens experienced a significant loss in the total energy

dissipation capacity. This is due to the volumetric mass loss and reduction in confined area of hysteretic loops (stress-strain loops). This is an important parameter for corroded structures located in seismic regions as they won't have enough energy dissipation capacity to withstand large earthquakes.

6) It is found that the fatigue behaviour of corroded bars with the effect of inelastic buckling has a significant path dependency. The results obtained in this paper are valid for low-cycle fatigue tests with constant symmetric strain amplitude. Therefore, there is need for further experimental study on corroded bars with the effect of inelastic buckling and different strain histories.

7) The experimental results reported in this paper show a significant scatter in the data compare to other experiments where test specimens were not corroded inside concrete. The comparison of the results suggests that accelerated corrosion technique, strain amplitude, load history and inelastic buckling are the most important parameters that affect the fatigue behaviour of corroded bars. To this end, there is need for further experimental testing to investigate these parameters. Nevertheless, the results reported in this paper provide an insight into this complex problem and provides a good set of experimental dataset to other researchers to use in the future research.

Acknowledgements

The experimental work is funded by the Earthquake Engineering Research Centre (EERC) at the University of Bristol. The first author would like to thank Dr Nicholas Alexander of the University of Bristol for providing valuable guidance during the course of this research. SEM studies were carried out in the Chemistry Imaging Facility with equipment funded by University of Bristol and EPSRC (EP/K035746/1). Any findings, opinions and recommendations provided in this paper are only based on the author's view.

References

[1] El-Bahy A, Kunnath SK, Stone WC and Taylor AW. Cumulative Seismic Damage of Circular Bridge Columns: Benchmark and Low-Cycle Fatigue Tests. ACI Struct J 1999; 96 (4): 633-643.

[2] Lehman DE, Moehle JP. Seismic performance of well-confined concrete columns. PEER Research Report 2000; University of California at Berkeley.

[3] Ou Y, Tsai L and Chen H. Cyclic performance of large-scale corroded reinforced concrete beams. Earthq Eng Struct D 2011; 41: 592-603.

[4] Meda A, Mostosi S, Rinaldi Z, Riva P. Experimental evaluation of the corrosion influence on the cyclic behaviour of RC columns. Eng Struct 2014; 76: 112-123.

[5] Ma Y, Che Y and Gong J. Behavior of corrosion damaged circular reinforced concrete columns under cyclic loading. Constr Build Mater 2012; 29: 548–556.

[6] Mander JB, Panthaki FD, Kasalanati A. Low-cycle fatigue behavior of reinforcing steel. J Mater Civil Eng 1994; 6 (4): 453-468.

[7] Chang GA, Mander JB. Seismic energy based fatigue damage analysis of bridge columns: Part I – Evaluation of seismic capacity. Technical report NCEER-94-0006, 1994.

[8] Brown J, Kunnath Sk. Low-cycle fatigue failure of reinforcing steel bars. ACI Mater J 2004; 101 (6): 457-466.

[9] Higai T, Nakamura H and Saito S. Fatigue failure criterion for deformed bars subjected to large deformation reversals. ACI SP 237-4 2006; 237: 37-54.

[10] Hawileh RA, Abdalla JA, Oudah F and Abdelrahman K. Low-cycle fatigue life behaviour of BS 460B and BS B500B steel reinforcing bars. Fatigue Fract Eng M 2010; 33: 397-407. (39).

[11] Kashani MM, Barmi AK and Malinova VS. Influence of inelastic buckling on low-cycle fatigue degradation of reinforcing bars. Constr Build Mater 2015; Under review.

[12] Apostolopoulos CA. Mechanical behavior of corroded reinforcing steel bars S500s tempcore under low cycle fatigue. Constr Build Mater 2007; 21: 1447–1456.

[13] Hawileh RA, Abdalla JA, Al Tamimi A, Abdelrahman K and Oudaha F. Behavior of corroded steel reinforcing bars under monotonic and cyclic loadings. Mech Adv Mater Struct 2011; 18:218–224.

[14] Kashani MM, Crewe AJ and Alexander NA. Nonlinear stress-strain behaviour of corrosion-damaged reinforcing bars including inelastic buckling. Eng Struct 2013; 48: 417–429.

[15] Kashani MM, Crewe AJ and Alexander NA. Nonlinear cyclic response of corrosion-damaged reinforcing bars with the effect of buckling. Constr Build Mater 2013; 41: 388-400.

[16] Kashani MM. Seismic Performance of Corroded RC Bridge Piers: Development of a Multi-Mechanical Nonlinear Fibre Beam-Column Model, PhD Thesis 2014; University of Bristol.

[17] Kashani MM, Crewe AJ, Alexander NA. Use of a 3D optical measurement technique for stochastic corrosion pattern analysis of reinforcing bars subjected to accelerated corrosion. Corros Sci 2013; 73: 208–221.

[18] Kashani MM, Lowes LN, Crewe AJ and Alexander NA. Finite element investigation of the influence of corrosion pattern on inelastic buckling and cyclic response of corroded reinforcing bars. Eng Struct 2014; 75: 113-125.

[19] Apostolopoulos Ch Alk, Michalopoulos D. Effect of corrosion on mass loss, and high and low cycle fatigue of reinforcing steel. J Mater Eng Per 2006; 15 (6): 742-749.

[20] Apostolopoulos CA, Papadakis VG. Consequences of steel corrosion on the ductility properties of reinforcement bar. Constr Build Mater 2008; 22 (12): 2316-2324.

[21] BS 4449-2005 +A2. Steel for the reinforcement of concrete - Weldable reinforcing steel - bar, coil and decoiled product – Specification; 2009.

[22] ASTM G1-03 Standard Practice for preparing, cleaning, and evaluating corrosion test specimens, ASTM Int'l 2011.

[23] Manson SS. Fatigue: A complex subject-Some simple approximations. Exp Mech 1965; 5 (7): 193–226.

[24] Kashani MM, Lowes LN, Crewe AJ and Alexander NA. Phenomenological hysteretic model for corroded reinforcing bars including inelastic buckling and low-cycle fatigue degradation. Comput Struct, Accepted for publication.

[25] OpenSees, the Open System for Earthquake Engineering Simulation. PEER 2014; University of California, Berkeley.

[26] Apostolopoulos C, Demis S, Papadakis V. Chloride-induced corrosion of steel reinforcement -mechanical performance and pit depth analysis. Constr Build Mater 2013; 38: 139-146.

Appendix A. Low-cycle fatigue test results

Table A1. Low-cycle fatigue test results of corroded bars with L/D = 5

Mass Loss (ψ) (%)	Amplitude (ε_a)	Frequency (Hz)	Total Time (s)	Number of Half-cycles to Failure ($2N_f$)	Normalised Mean Dissipated Energy (E'_i/E_t)
0.00	0.01	0.125	3733.14	933	1.00
14.03	0.01	0.125	1102.30	276	0.36
14.65	0.01	0.125	1557.20	389	0.49
0.00	0.02	0.0625	1124.69	141	1.00
12.86	0.02	0.0625	1077.20	135	0.95
13.31	0.02	0.0625	1112.90	139	0.92
20.10	0.02	0.0625	645.24	81	0.59
34.20	0.02	0.0625	920.08	115	0.78
0.00	0.03	0.0417	607.52	51	1.00
11.00	0.03	0.0417	391.81	33	0.55
16.06	0.03	0.0417	680.84	57	1.01
21.33	0.03	0.0417	503.46	42	0.62
34.9	0.03	0.0417	152.40	13	0.05
0.00	0.04	0.0313	527.26	33	1.00
15.58	0.04	0.0313	424.09	27	0.65
18.95	0.04	0.0313	384.80	24	0.63
20.69	0.04	0.0313	485.50	30	0.74
33.69	0.04	0.0313	389.27	24	0.44

Table A2. Low-cycle fatigue test results of corroded bars with L/D = 10

Mass Loss (ψ) (%)	Amplitude (ε_a)	Frequency (Hz)	Total Time (s)	Number of Half-cycles to Failure ($2N_f$)	Normalised Mean Dissipated Energy (E'_i/E_t)
0.00	0.01	0.125	887.13	222	1.00
11.22	0.01	0.125	694.25	174	0.70
15.37	0.01	0.125	709.67	177	0.67
18.76	0.01	0.125	621.08	155	0.59
37.66	0.01	0.125	716.76	179	0.38
0.00	0.02	0.0625	409.95	51	1.00
11.49	0.02	0.0625	502.23	63	1.01
13.91	0.02	0.0625	483.93	60	1.07
22.47	0.02	0.0625	388.88	49	0.76
35.71	0.02	0.0625	597.01	75	0.86
0.00	0.03	0.0417	298.79	25	1.00
11.22	0.03	0.0417	296.84	25	0.91
12.37	0.03	0.0417	508.18	42	1.29
23.90	0.03	0.0417	318.92	27	0.74
29.81	0.03	0.0417	511.02	43	1.08
0.00	0.04	0.0313	267.21	17	1.00
9.60	0.04	0.0313	237.64	15	0.45
16.03	0.04	0.0313	392.84	25	0.59
23.41	0.04	0.0313	451.94	28	0.51
25.45	0.04	0.0313	171.04	11	0.23

Table A3. Low-cycle fatigue test results of corroded bars with L/D = 15

Mass Loss (ψ) (%)	Amplitude (ε_a)	Frequency (Hz)	Total Time (s)	Number of Half-cycles to Failure ($2N_f$)	Normalised Mean Dissipated Energy (E'_i/E_t)
0.00	0.01	0.125	576.23	144	1.00
11.76	0.01	0.125	573.13	143	0.94
16.51	0.01	0.125	486.06	122	0.72
20.48	0.01	0.125	316.55	79	0.46
33.65	0.01	0.125	1013.26	253	1.09
0.00	0.02	0.0625	426.05	53	1.00
11.66	0.02	0.0625	310.38	39	0.59
13.06	0.02	0.0625	453.39	57	0.86
17.06	0.02	0.0625	489.00	61	0.91
34.22	0.02	0.0625	1588.86	199	2.05
0.00	0.03	0.0417	393.49	33	1.00
12.13	0.03	0.0417	389.55	32	0.95
13.21	0.03	0.0417	247.51	21	0.57
23.60	0.03	0.0417	295.32	25	0.67
24.49	0.03	0.0417	265.97	22	0.55
0.00	0.04	0.0313	363.16	23	1.00
14.26	0.04	0.0313	265.04	17	0.71
14.32	0.04	0.0313	485.75	30	1.05
20.30	0.04	0.0313	450.56	28	1.00
24.37	0.04	0.0313	450.89	28	0.99

Research Highlights

1. Influence of corrosion and buckling on hysteretic loops of corroded bars.
2. Impact of corrosion on cyclic stress degradation of bars.
3. Combined Impact of corrosion and buckling on number of cycles to failure.
4. Combined influence of corrosion and buckling on fracture mechanism.